A Motion-Artifact Tracking and Compensation Technique for Dry-Contact EEG Monitoring System

Jingyi Song[1,2], Tuo Shan[1], Shuang Zhu[1], and Yun Chiu[1]
[1]Texas Analog Center of Excellence, University of Texas at Dallas, Richardson, TX, USA
[2]College of Electronic Science & Engineering, Jilin University, Changchun, Jilin, China

***Abstract*—A digital online technique for motion artifact (MA) tracking and compensation is reported for electroencephalogram (EEG) monitoring using dry-contact electrodes. A safe, low-level pseudorandom noise (PN) signal is driven to the body through a reference electrode as a test signal to measure the bio-potential acquisition-path gain (APG) of the electrode-tissue interface (ETI). The measurement result is then utilized by a digital-domain gain compensator to act in the opposite way to the MA-induced APG variation, thereby compensating the multiplicative motion artifact (MMA) in real time. The remaining baseline wander or additive motion artifact (AMA) is treated by a digital high-pass filter (HPF). The interference of the test signal to the EEG signal acquisition is negligible in this technique due to the nearly white spectrum of the PN signal.**

***Keywords*—BCI; EEG; ETI; motion artifact; MMA; AMA**

I. Introduction

Bio-potential acquisition using disposable dry-contact electrodes is quickly arising as a contender to conventional wet-electrode sensing techniques in clinical applications, brain-computer interfaces, and gaming devices. One critical problem in such a system is the impedance and baseline variations of the capacitively coupled electrode-tissue interface (ETI) layers due to muscular activities, e.g., eye blinking, breathing, etc., commonly known as motion artifacts (MA). Left untreated, MA poses a significant challenge to the quality of the recorded bio-signals—often manifested in the form of distortion and/or baseline drift—even when the sensor analog frontend electronics (AFE) is well designed and operate normally.

Conventionally, ETI is modeled as a parallel RC structure in series with the half-cell potential and the tissue resistance, as shown in Fig. 1(*a*) [1]. Therefore, the MA-induced ETI variations are usually characterized as impedance—resistance and capacitance—variations and a time-varying offset voltage based on the lumped circuit model. Most of the prior works in this area are focusing on rejecting the offset or baseline wander using a high-pass filter (HPF) [2-4]. A few recent works also reported ETI impedance-variation detection and tracking techniques [5-6]. However, to our best knowledge, no existing technique has been reported to stabilize or compensate the ETI characteristic variations in presence of MA.

This work is supported by Semiconductor Research Corporation (SRC) through Texas Analog Center of Excellence at the University of Texas at Dallas (Task ID: 1836.103).

Yun Chiu is the correspondence author (E-Mail: chiu.yun@utdallas.edu).

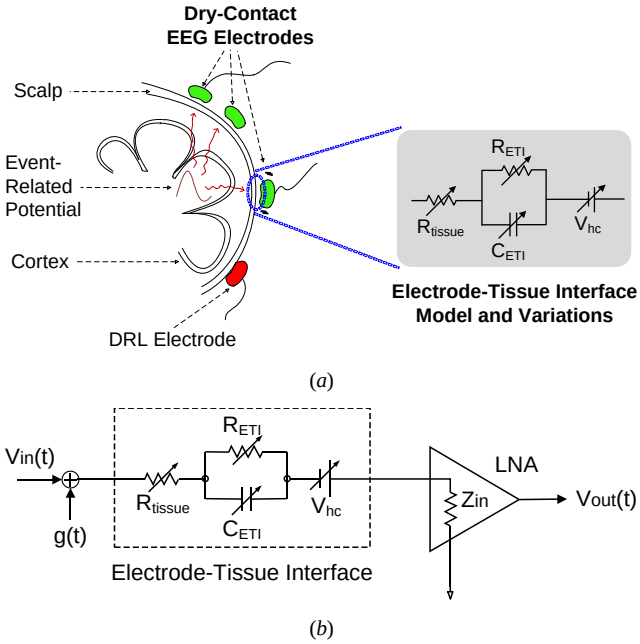

Figure 1. (*a*) Equivalent circuit model of ETI and MA-induced ETI impedance variation and baseline wander in EEG recording and (*b*) bio-potential acquisition path including the ETI and a low-noise amplifier (LNA) in AFE. $g(t)$ is the injected test signal to measure APG.

In this work, a novel MA tracking and compensation technique is reported for seamless integration with the AFE of dry-contact bio-sensing devices to stabilize the ETI response. A low-level pseudorandom noise (PN) signal, which abides the safety standard of the American Association for the Advancement of Medical Instrumentation, is driven to the body and propagates through the ETI as a test signal, i.e., the $g(t)$ shown in Fig. 1(*b*), to measure the signal acquisition-path gain (APG) of the ETI. The injected PN signal is recorded at the same time with and in exactly the same way as the bio-potentials. By comparing the recorded PN with its original known form via digital correlation, the impairments due to the multiplicative MA (MMA) can be assessed; this information in turn is utilized to direct a digital gain compensator to perform counter-moves to neutralize the APG variations. When combined with baseline filtering, the technique will lead to stable, distortion-free bio-potential recordings in presence of MA.

We tested the proposed technique on four healthy human subjects with real-time EEG tasks. The four student partici-

pants, one female and three males, were recruited from the Texas Analog Center of Excellence at UT Dallas. Their average age was 26 (ranging from 23 to 27). All subjects were healthy without any history of head injury or neurological disorders. Experimental data in both time and frequency domains show significant improvements in the detection of alpha waves after MMA compensation.

II. Classification of Motion Artifacts

A simple network analysis of the equivalent circuit model of the bio-signal acquisition path shown in Fig. 1(*b*) results in the following voltage transfer function of the AFE.

$$V_{out}(t) = A(t)\cdot\left[V_{in}(t) + g(t) + V_{hc}(t)\right] + noise, \quad (1)$$

$$A(t) = \frac{Z_{in}}{Z_{in} + Z_{ETI}(t)},\ Z_{ETI}(t) = R_{tissue} + \frac{R_{ETI}}{1 + sR_{ETI}C_{ETI}}, \quad (2)$$

where $V_{in}(t)$ is the input bio-signal, $g(t)$ is the injected test signal, $V_{out}(t)$ is the AFE output (a distorted version of the summation of the input bio-signal and the test signal), $V_{hc}(t)$ is a half-cell potential existing in the ETI due to piezoelectric effect between the skin and electrode. The time-varying half-cell potential gives rise to the baseline wander, which we term the additive motion artifact (AMA). In (2), Z_{in} is the input impedance of the low-noise amplifier (LNA), which is often in the range of 100 GΩ and fixed over time. Thus, the variation of the ETI impedance $Z_{ETI}(t)$ results straight in a magnitude distortion of $V_{in}(t)$, characterized by the APG $A(t)$ experienced by both $V_{in}(t)$ and $g(t)$. We define $A(t)$ as the multiplicative motion artifact (MMA). In practice, both AMA and MMA degrade the signal quality of recording, particularly when dry-contact electrodes are used. However, the fundamental difference between AMA and MMA lies in the fact that AMA is a linear effect (i.e., additive noise) whereas MMA is a nonlinear distortion. Therefore, the MMA distortion cannot be simply eliminated by linear signal processing such as filtering.

III. Proposed MA Compensation Technique

We propose an online tracking and adaptive compensation technique to treat MMA. The system block diagram is shown in Fig. 2. A low-level PN signal $g(t)$ is driven to the body and received by the EEG electrodes at the same time the bio-signals are received (the solid path). Upon proper synchronization, the received PN sequence is correlated to its original form (the dashed path) and averaged over time, yielding

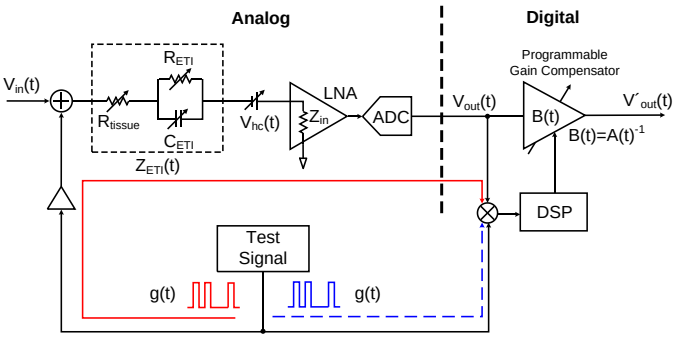

Figure 2. The signal-acquisition path of a typical EEG recording device with the proposed technique of MMA tracking and compensation.

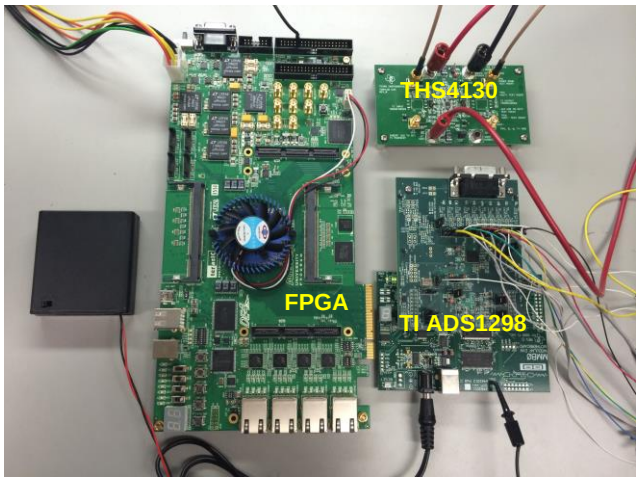

Figure 3. Hardware setup for in-house EEG monitoring.

$$\begin{aligned}&\overline{V_{out}(t)\cdot g(t)}\\ &= \cancel{\overline{A(t)\cdot V_{in}(t)\cdot g(t)}} + \overline{A(t)\cdot g(t)\cdot g(t)}\\ &+ \cancel{\overline{A(t)\cdot V_{hc}(t)\cdot g(t)}} + \cancel{\overline{noise\cdot g(t)}}\\ &= \overline{A(t)},\end{aligned} \quad (3)$$

due to the self-correlation property of the PN. Equation (3) indicates that a time average of $A(t)$ can be detected using this procedure. Thus, by choosing a proper time duration of the correlation process and assuming that $A(t)$ varies slowly over time, the technique results in a direct detection of the MMA. Once $A(t)$ is known, a programmable gain compensator with its gain $B(t)$ set to $A(t)^{-1}$ can be employed to neutralize the effect of MMA in the digital domain, as shown in Fig. 2. The post-compensation output $V'_{out}(t)$ will be a distortion-free, linear function of $V_{in}(t)$.

In addition, due to its low amplitude and almost white spectrum, the residual PN signal in the output after MMA compensation usually does not need to be removed, although it can be done by employing an adaptive noise cancellation loop [7]. In the experimental results disclosed in Section IV, such residual PN cancellation loop is not implemented.

Once MMA is treated, the remaining AMA or baseline wander can be dealt with using a digital HPF with a low cutoff frequency. In our experiment, this frequency is set to 1 Hz. Note that the MMA compensation needs to be applied before the HPF according to Equation (1).

In summary, in the proposed approach we avoided a direct measurement of the ETI impedance as commonly done in prior works. Instead, we focus on the consequences of the ETI variations, i.e., MMA and AMA, and track and compensate them effectively using adaptive digital techniques. The method is in-situ and operates in the background (online) with minimal or negligible interference to the normal foreground biopotential recording process.

IV. Experimental Setup and Results

The hardware setup of our in-house EEG monitoring system is shown in Fig. 3. The AFE signal-acquisition functions

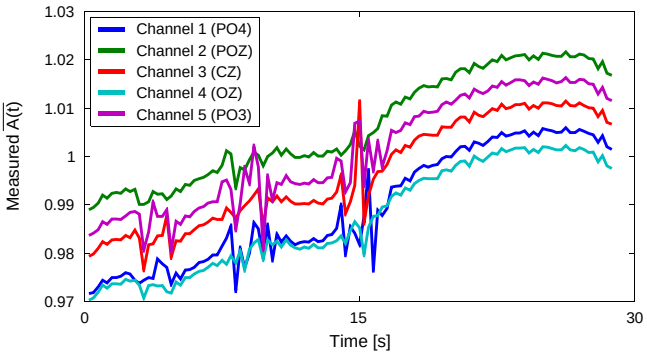

Figure 4. Measured APG variations of the AFE during EEG monitoring. The three busy MMA incidents during the first 15 seconds of recording correspond to three head movements (nodding) the subject performed.

are performed by the Texas Instruments (TI) ADS1298 bio-signal measurement board with integrated 24-bit analog-to-digital converters (ADCs). All digital processing is executed in an Altera DE4 FPGA board including the PN generation and data post-processing. The generated test PN signal passes through a voltage divider and is driven to the body using the TI THS4130 evaluation board of operational amplifiers.

In our EEG measurements, there are five dry-contact electrodes placed on the scalp of the subject, using the standard 10-20 electrode. The electrode positions are CZ, POZ, OZ, PO3, and PO4 in our experiments. Another electrode is attached to the wrist for test signal injection. No special skin abrasion or preparation was performed before recording. In the first experiment, the subject was asked during the initial 15 seconds to nod his/her head 3 times (i.e., once every 5 seconds) and then remain as steady as possible for the next 14 seconds. During the recording, the subject was also asked to maintain a relatively stable wrist position. The measured average APG or $\overline{A(t)}$ of Equation (3) during the 29-second recording is plotted in Fig. 4. The head movement resulted in three fast APG variations or MMA (once every 5 seconds), which ride on top of a slowly rising gain ramp throughout the recording whose origin is not clear. The sample rate in this experiment is 8 kHz. The PN sequence has a length of 8192 samples. The time duration of the moving average $\overline{A(t)}$ measurement is also 8192 samples, equal to the PN length. The experiment described next employs the same setup.

During the second measurement, the alpha wave was selected to be the target EEG signal for observation and the subject was asked to close and open his/her eyes during the recording. The subject was asked to open his/her eyes in the first 5 seconds and then close eyes till the end. During the whole 11 seconds of recording, the subject was asked to nod his/her

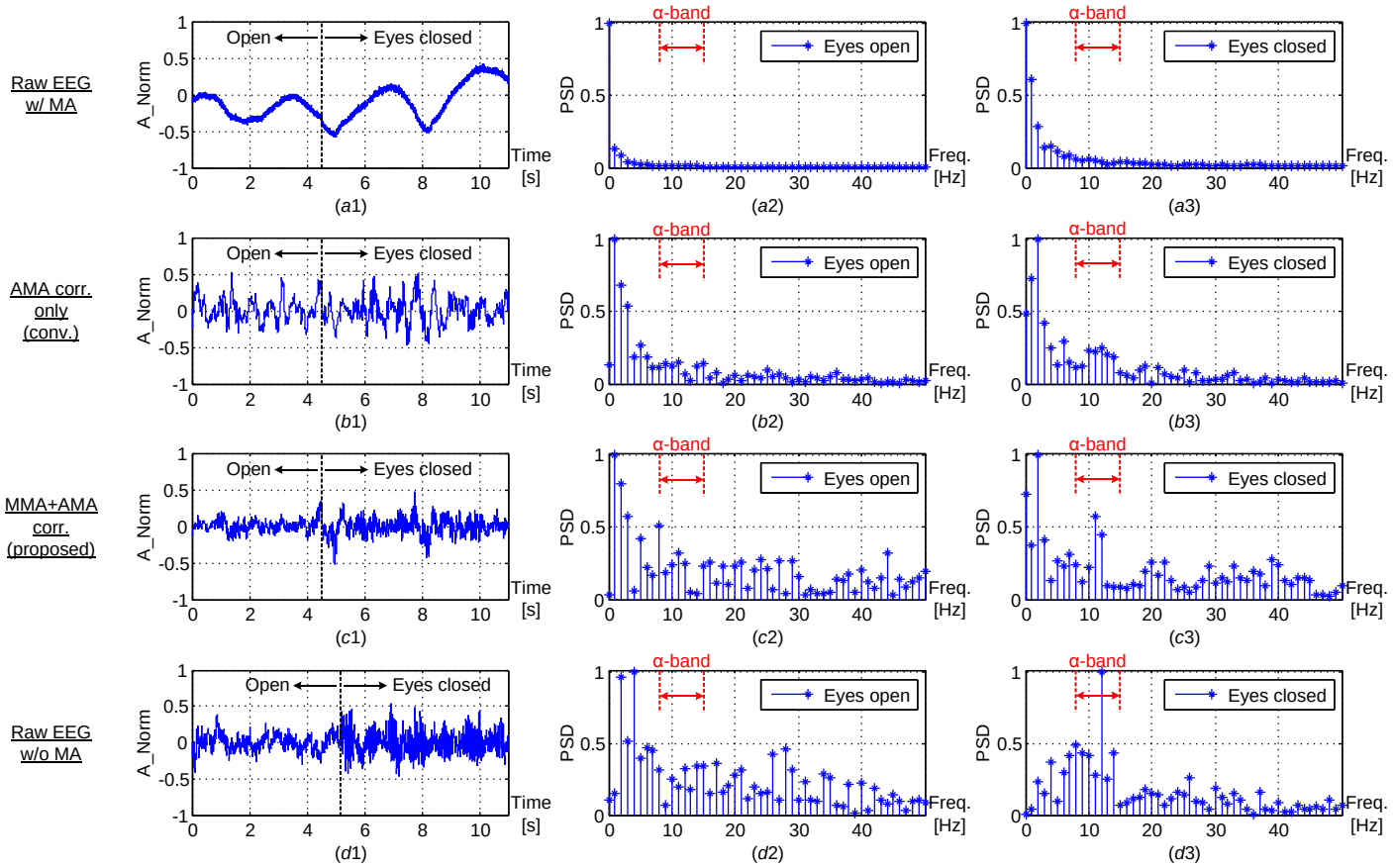

Figure 5. **Column one**: (*a*1) recorded raw EEG waveform with MA, (*b*1) the recording of *a*1 processed by a 1-Hz HPF, (*c*1) the recording of *a*1 processed using the proposed MMA technique first and then by the HPF, and (*d*1) recorded raw EEG waveform without MA; **Column two**: the spectrum of the first 4 seconds (eyes open) of the waveform in (*a*2) *a*1, (*b*2) *b*1, (*c*2) *c*1, and (*d*2) *d*1; **Column three**: the spectrum of the last 6 seconds (eyes closed) of the waveform in (*a*3) *a*1, (*b*3) *b*1, (*c*3) *c*1, and (*d*3) *d*1. All time-domain waveforms are single measurement results, while the spectra were all computed and averaged over ten identical measurements.

head 3 times to induce MAs experienced by the scalp electrodes. The normalized time-domain EEG waveforms and the spectra corresponding to the first 4-5 seconds (eyes open) and the rest 6-7 seconds (eyes closed) are computed and plotted in Fig. 5. Note that the first row of Fig. 5 (*a*1-*a*3) corresponds to the raw EEG waveform with MA, the second row (*b*1-*b*3) corresponds to the same result after conventional baseline (or AMA) filtering using a digital HPF with a 1-Hz cutoff frequency, the third row (*c*1-*c*3) also corresponds to the same result but after the proposed MMA compensation first and then baseline filtering, and the last row (*d*1-*d*3) corresponds to the raw EEG waveform recorded without MA, in which the subject was asked to remain as still as possible during the recording. In addition, in columns two and three (*a*2-*d*2 and *a*3-*d*3) of Fig. 5, each spectrum was computed and averaged over ten identical recordings to improve the signal-to-noise ratio.

The first noticeable phenomenon in *a*1 is the three periods of baseline fluctuation caused by the periodic head movement of the subject. The frequency of this AMA is ~0.27 Hz, which is rejected by the 1-Hz HPF as shown in *b*1 and *c*1. Secondly, while the spectra in the second column (*a*2-*d*2) corresponding to the EEG recording with eyes open all lack obvious alpha-band (8-15 Hz) content, the spectrum in *a*3 corresponding to the case with eyes closed but in presence of MA also lacks strong alpha-band content due to the MMA distortion—note that this is not simply due to the masking effect of the large baseline content close to DC because the alpha-band spectral content is still not obvious even after baseline filtering alone as shown in *b*3. However, once both MMA and AMA treatments are administered, the alpha-band arose from the noise floor as illustrated in *c*3. The comparison between the spectra plotted in *b*3 (baseline filtering alone), *c*3 (the proposed MMA compensation and then baseline filtering), and *d*3 (the MA-free case) demonstrates the significance of MMA and the proposed technique in assisting the detection of alpha wave in presence of MA during this experiment. A similar observation can also be made in the time domain by comparing the EEG waves shown in *b*1 (with baseline filtering alone) and *c*1 (after both MMA and AMA treatments)—the filtering-alone result still displays fast up-and-down segments that cannot be removed by a low-cutoff HPF, i.e., they are the distortion artifacts caused by the MMA.

In addition, Fig. 6 summarizes the normalized spectra in the alpha-band (8-15 Hz) for the three tests reported above. In the figure, all ten individual measurements are marked with hollow 'square', 'triangle', and 'circle' symbols, corresponding to the raw, post-AMA correction, and post-MMA+AMA correction recordings, respectively, and the solid symbols and curves represent the spectral content averaged over the ten datasets. We can observe that there is no significant spectral peak in the raw dataset (dot-dashed curve with square symbols), whereas after the AMA correction (dashed curve with triangular symbols), the alpha-band power spectral density (PSD) is enhanced—for instance, the PSD at 11 Hz is improved by 0.168 (from 0.056 to 0.224) and the one at 12 Hz is improved by 0.195 (from 0.050 to 0.245). In contrast, the PSD

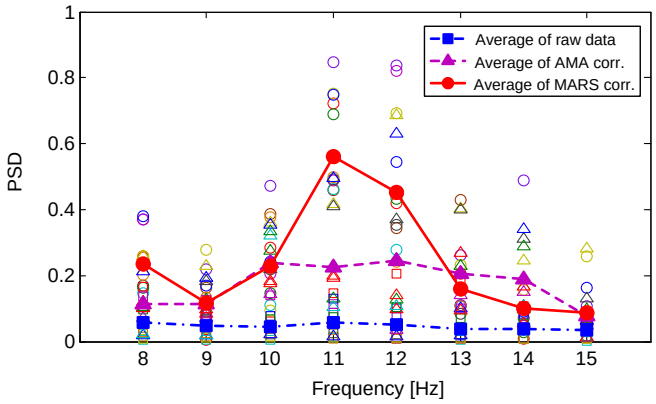

Figure 6. Individual and average PSD (within alpha-band) of the raw EEG recording, post-AMA, and post-MMA+AMA results. Improvements are most obvious at 11 Hz and 12 Hz for this subject.

computed using the proposed technique (i.e., MMA+AMA) revealed two obvious peaks at 11 Hz and 12 Hz—the average PSD values (solid curve with circular symbols) show that the two maximum improvements of 0.505 (from 0.056 to 0.561) and 0.401 (from 0.050 to 0.451) occur at 11 Hz and 12 Hz, respectively. From these measurement results, we conclude that the MMA correction is essential in this experiment, and the proposed MARS technique works better than the conventional AMA-alone technique for stabilizing the ETI response.

V. Conclusion

The multiplicative and additive aspects of motion artifacts due to ETI variations in EEG recording are clarified. A novel electronic technique is proposed for online tracking and compensation of MMA distortion to improve the reliability of biopotential recording devices using dry electrodes. Alpha-wave recording was conducted and the measurement results demonstrate the efficacy of the proposed technique.

References

[1] Y. M. Chi *et al.*, "Dry-contact and non-contact biopotential sensors," *IEEE Reviews in Biomedical Engineering*, pp. 106–119, Mar. 2010.

[2] H. Nolan *et al.*, "Acquisition of human EEG data during linear self-motion on a Stewart platform," *IEEE EMBS Conf. on Neural Eng.*, pp. 585–588, 2009.

[3] H. Nolan *et al.*, "Motion P3 demonstrates neural nature of motion ERPs," *IEEE EMBS Boston*, pp. 3884–3887, 2011.

[4] Y. Lin *et al.*, "Assessing the quality of steady-state visual-evoked potentials for moving humans using a mobile electroencephalogram headset," *Frontiers in Human Neuroscience*, vol. 8, pp. 1–10, Mar. 2014.

[5] S. Mitra *et al.*, "A 700μW 8-channel EEG/contact-impedance acquisition system for dry-electrodes," in *IEEE Symp. VLSI Circuits, Dig. Tech. Papers*, pp. 68–69, 2012.

[6] R. Yazicioglu *et al.*, "A 30μW analog signal process ASIC for biomedical signal monitoring," in *IEEE Int. Solid-State Circuits Conf., Dig. Tech.Papers*, pp. 124–126, 2010.

[7] M. Yelderman *et al.*, "ECG enhancement by adaptive cancellation of electrosurgical interference," *IEEE Trans. Biomed. Eng.*, vol. BME-30, pp. 392–398, 1983.